Latency of the Pupil Light Reflex: Sample Rate, Stimulus Intensity, and Variation in Normal Subjects

Oliver Bergamin[1,2] *and Randy H. Kardon*[1]

Purpose. To investigate the clinical usefulness of the latency of the pupil light reflex by optimizing its measurement, characterizing its variability, and determining the sensitivity of pupil latency as a function of stimulus input in normal subjects.

Methods. Computerized binocular infrared pupillography was performed in 14 eyes of seven healthy subjects. Pupils were recorded simultaneously at 60 and 1000 Hz. Each eye was alternatively stimulated eight times for 50 ms every 2.5 seconds, increasing by 0.5 log units over a 2.0-log-unit range. To determine intersubject and intereye variability, 98 eyes of 49 healthy subjects were recorded at 60 Hz over a 3.0-log-unit range (15° radius stimulation, four repetitions at each intensity).

Results. Accuracy and resolution of latency were limited by the number of light reflexes used to estimate the average latency and were significantly affected by sampling rate when the number of reflexes recorded was fewer than four. Binocular recording and interpolation of the 60-Hz recording to 300 Hz added resolution to the latency. Biological variability contributed more to interindividual variability than did measurement variability. The range of intereye afferent asymmetry of latency in normal subjects was only between 8.3 and 35 ms—less with brighter stimulus intensity.

Conclusions. An optimal method for determination of the onset of the pupil light reflex was devised that consisted of filtering, interpolation of pupil recordings, and analysis of the first and second derivative of the pupil movement. Most of the variability in latency as a function of intensity in normal subjects was due to interindividual variation and latency was well matched between the two eyes of the subjects. (*Invest Ophthalmol Vis Sci.* 2003;44:1546–1554) DOI:10.1167/iovs.02-0468

The pupil latency—the precise definition of the onset of pupil movement in reaction to the onset of a stimulation by light—can objectively reveal delays in visual processing proportional to the amount of afferent damage,[1] similar to the visual evoked potential (VEP)[2–5] and the Pulfrich phenomenon.[6–9] In addition, latency, compared with amplitude measurements, may be less affected by mechanical properties of the iris that are known to constrain the movement of the pupil that occurs after the onset of contraction.[10] Loewenfeld has provided evidence that pupil latency may be less variable than amplitude measurements for assessing afferent input to the eye and thoroughly reviewed the literature on this topic up until 1990.[11] Previous studies have shown that pupil latency and cycling time can be delayed in patients with afferent diseases, such as demyelinating disease,[12–14] Leber hereditary optic neuropathy,[15] amblyopia,[16,17] and optic atrophy,[18] and also in efferent pupil disorders that affect the autonomic nerves to the iris, such as diabetes.[19,20]

Compared with the VEP, in which a clear trough can be identified as the end point of the latency period, the onset of contraction of the pupil in response to light (pupil light reflex) is not as simple to determine. The action of the smooth pupil sphincter muscle does not cause an abrupt change in the pupil tracing. Despite previous studies of pupil latency,[21–27] there is still no agreement on the optimal method for its measurement,[24,28–34] and there is a paucity of information on the variability of latency between eyes and among normal subjects. In a previous study,[33] we have defined the onset of the pupil light reflex as the time at which the absolute acceleration is greatest (second derivative), but this method has not been investigated in detail.

The purpose of this study was to define the onset of the pupil light reflex more precisely, to determine an optimal method for measurement of pupil latency, to determine whether sampling the pupil at higher rates would improve latency accuracy and resolution, and to further understand the biological and measurement variability of pupil latency in normal eyes. This study was intended to provide a basis for the measurement of the latency of the pupil light reflex in healthy eyes that can be used in future studies to evaluate diseased eyes.

Methods

The study was conducted according to the tenets of the Declaration of Helsinki. Seven normal volunteers, two men and five women (mean age: 34 years; range: 26–45), were included. The second set of 49 normal subjects, 23 men, 26 women (mean age, 32 ± 10 years; range, 22–47), were used to apply the optimal method of measurement of latency to characterize the intereye and intersubject variability. Normal subjects tested by pupillography were not receiving any medications known to influence the pupil light reflex. All the normal subjects had visual acuity of at least 20/20 in each eye, normal stereovision, normal findings in slit lamp and fundus examinations, and normal standard threshold perimetry (program 24-2; Zeiss Humphrey Systems, Dublin, CA).

Pupillometer

A computerized binocular infrared video pupillometer (developed by Tom Cornsweet; Visual Pathways, Inc., Prescott, AZ) was used to record pupil responses in the seven subjects over a range of stimulus

From the [1]Department of Ophthalmology and Visual Sciences and Veterans Administration Hospital, University of Iowa, Iowa City, Iowa; and the [2]Department of Ophthalmology, University Hospital of Zürich, Zürich, Switzerland.

Supported by the Swiss National Science Foundation, the Freiwillige Akademische Gesellschaft, Basel, Switzerland; the Roche Research Foundation, Basel, Switzerland; an unrestricted grant from Research to Prevent Blindness, New York, New York; a grant from Zeiss-Humphrey Corp., Dublin, California; and a Merit Review and Career Development Award from the Veterans Administration, Washington, DC (RHK). RHK is the recipient of a Lew Wasserman Scholar Award from Research to Prevent Blindness.

Submitted for publication May 15, 2002; revised October 17, 2002; accepted November 26, 2002.

Commercial relationships policy: N.

The publication costs of this article were defrayed in part by page charge payment. This article must therefore be marked "*advertisement*" in accordance with 18 U.S.C. §1734 solely to indicate this fact.

Corresponding author: Randy H. Kardon, Department of Ophthalmology and Visual Sciences, University of Iowa Hospitals and Clinics, PFP, 200 Hawkins Drive, Iowa City, IA 52242-1091; randy-kardon@uiowa.edu.

Investigative Ophthalmology & Visual Science, April 2003, Vol. 44, No. 4

light intensities. The infrared pupillometer consists of a monochrome video graphics array (VGA) monitor with non-Maxwellian viewing optics used to present light stimuli to the subject, two identical systems for pupil tracking (one for each eye), and two charge-coupled device (CCD) cameras for recording the pupil response of each eye simultaneously.[35] The internal viewing monitor is driven in the *z*-axis toward or away from the patient by a stepper motor to change its optical distance from the eyes over a range of ±7.00 D of refractive error, so that the plane of the stimulus was at optical infinity for the subjects. The VGA monitor was synchronized at 60 Hz with the two video cameras (type VC62505T; Visual Pathways) used to record the right and left pupils with 0.025-mm resolution of pupil diameter. Stimuli presented by the VGA monitor were initiated at the beginning of the video half-frame synchronized with the two video cameras. The video output of each camera was processed in a circuit board that measured the horizontal diameter of the pupil. In addition, two infrared photodiode quadrant sensors placed in the optical pathway measured the total amount of reflected infrared light from the bright image of each pupil at a rate of 1000 Hz. The bright pupil image is a result of infrared light reflected back from the fundus and therefore is not influenced by iris color. The sum of the four quadrants' output for each pupil was sampled at 1000 Hz to estimate pupil size at a high rate, in addition to a simultaneous video recording of each pupil at 60 Hz.

The 49 normal subjects that participated for assessing the variability of pupil latency were measured with an earlier prototype binocular infrared pupillometer described previously with only the 60-Hz recording.[36–38] This pupillometer used Maxwellian view optics, recorded at 60 Hz only, and converged a bank of four green LED light sources imaged by Fresnel lenses as four squares of light subtending 30° diameter of visual field with a small red fixation point in the center of the four squares. In this instrument, the 30° square light stimulus was converged to a diameter of 1.5 mm in the plane of the pupil and kept centered in the pupil space by the use of tracking motors. There was no background light between stimuli.

Stimulus Paradigms

Full-field stimuli were alternatively presented to the right and left eyes for every condition with the newer prototype machine. In the first phase of the study, seven normal subjects were tested with each eye stimulated for eight cycles (50-ms stimulus every 2.5 seconds) at five stimulus intensities, separated by 0.5 log units over a 2.0-log-unit range (from 10-dB attenuation [100 asb, 31.9 cd/m^2] to 30-dB attenuation [1 asb, 0.319 cd/m^2]; stimulus radius, 23°). A septum divided the VGA monitor into right and left halves to stimulate the right and left eyes independently. The VGA monitor had a dark luminance of 0.1 cd/m^2, which is negligible. A fixation cross present in the VGA-generated image was always in the center of the visual field of the eye that was receiving the stimulus and was kept at a luminance that was easily seen during the stimulation and during the periods between stimuli. For every stimulus, the responses of the right and left pupils were recorded at both 60 and 1000 Hz simultaneously and analyzed off-line.

In the second phase of the study, the 49 normal subjects were measured with the older prototype machine (60-Hz collection only), at seven different intensities with four repetitions used in each cycle over a 3.0-log-unit range (from 0 dB attenuation [37,000 asb, 11,770 cd/m^2] to 30 dB attenuation [37 asb, 11.7 cd/m^2]; stimulus diameter, 30°).

Pupil Analysis

To achieve pupil diameter measured in millimeters, the raw bit data of the 60-Hz recording was divided by 78. The 1000-Hz measurement was calibrated by correlating the 1000-Hz raw data with the 60-Hz data. For each subject, the specific slope served as the multiplier to turn the 1000-Hz data into data expressed as pupil diameter.

The beginning of the pupil light reflex was defined as the time at which the greatest absolute acceleration in the tracing occurred. To achieve this goal, the signal-to-noise ratio was increased by minimizing the amplifier noise from the photodiode sensor that occurred in the

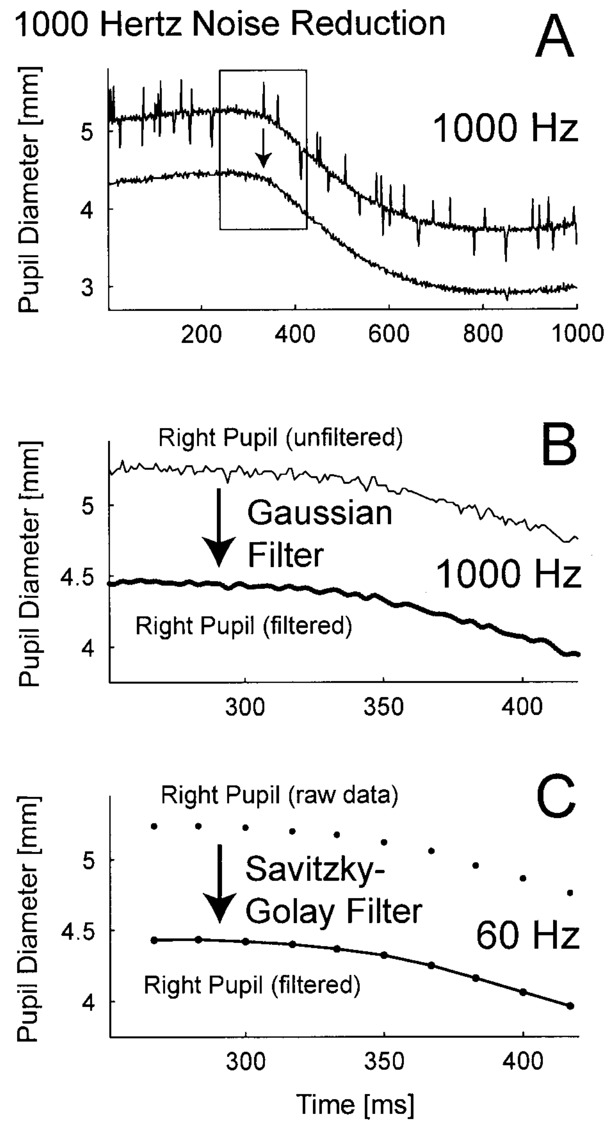

FIGURE 1. Reduction of measurement noise by removal of high-frequency spikes from the 1000-Hz right pupil trace (**A**). The portion of the 1000-Hz trace outlined by the *box* in (**A**) is shown in more detail in (**B**) and was next filtered with a Gaussian filter. The exact same portion of the right pupil light reflex shown in (**A**) and (**B**) that was recorded at 1000 Hz using a photodiode was also recorded simultaneously at 60 Hz, using a video signal, and is shown in (**C**). The 60-Hz recording was filtered with a Savitzky-Golay filter.[39]

1000-Hz raw data (Fig. 1A, top trace). Time points were omitted if the change in pupil size exceeded 0.1 mm/ms, on the assumption that the human pupil could not move faster. The high-frequency component was nonbiological and was caused by the noise emitted by the hardware and was present in recordings made from pharmacologically dilated and fixed pupils. The gaps from the eliminated time points were then linearly interpolated. The bottom trace in Figure 1A shows the result with the highest peaks removed and interpolated (subject FC). Eyelid blinks were then removed from the traces of both the 60- and 1000-Hz data sets separately, and time points were linearly interpolated.

Next, the 1000- and 60-Hz recordings each underwent a separate filtering procedure (Figs. 1B, 1C). For the 1000-Hz recording, a moving Gaussian filter with a 9-number base (4-ms width on each side of the center-weighted time point) was applied once, resulting in a minimal smoothing of the tracing, as shown in Figure 1B. The frequency response curve of the 9-point Gaussian filter showed that this filter

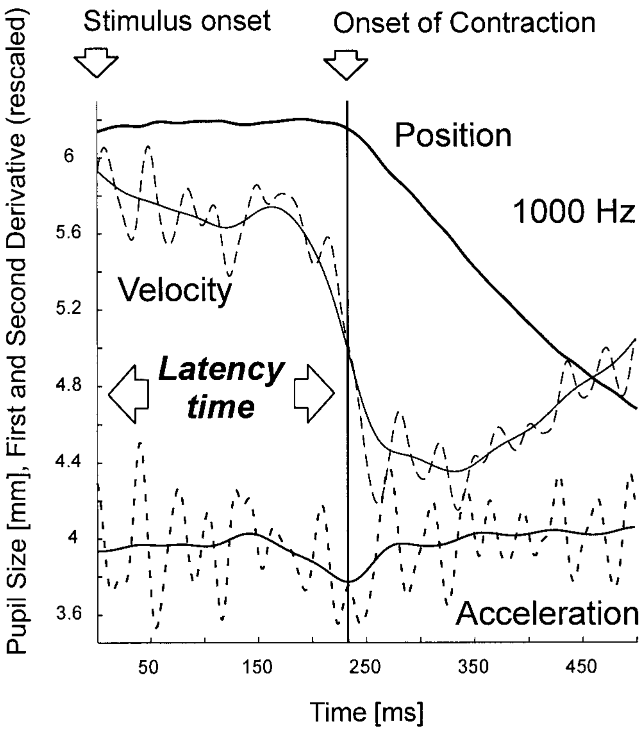

FIGURE 2. Determination of the onset of pupil contraction by using velocity and acceleration analysis. A single contraction phase of a pupil light reflex is shown, and superimposed are the velocity and acceleration (unfiltered traces are *dashed*). Only the velocity data have been additionally filtered (*solid line*). The portion of the velocity trace where maximum slope occurred is the time when the acceleration trace showed a well-defined trough, and this was the time when the onset of pupil contraction was defined (*vertical line*).

allowed 90% of a 50-Hz signal, 60% of a 107-Hz signal, and 30% of a 165-Hz signal to pass at the 1000-Hz sampling rate. For the 60-Hz video recording, a 5-point second-order polynomial moving Savitzky-Golay filter[39] was used (Matlab, ver. 5.3, function SAVGOL3.m, ver. 2.3, programmed by Thomas Haslwanter, Zurich, Switzerland; the MathWorks, Inc., Natick, MA), as shown in Figure 1C. The Savitzky-Golay filter allowed 90% of a 10.5-Hz signal, 60% of a 15.8-Hz signal, and 30% of a 19.2-Hz signal to pass in the 60-Hz sampling rate. Therefore, both filters are more effective in gradually reducing higher-frequency components. A digital filter with a sharp cutoff that provides an accurate measure of frequency bandwidth was not used, because such an arbitrary determination would have needed further justification. A 4-point 60- to 300-Hz interpolation was also applied to the 60-Hz data, by applying a cubic spline function to the 60-Hz position and velocity tracings. The resultant 300-Hz data served as an additional sampling rate to be analyzed. We also reduced the 1000-Hz data as close as possible to the 60-Hz data for direct comparison. Every 17th time point was preserved from the smoothed and filtered 1000-Hz position data, resulting in a measurement frequency of 58.8 Hz. To deduce the onset of the pupil contraction, the second derivative (acceleration) of the position tracing was calculated by taking the derivative of the velocity tracing after the tracing was filtered (described later). Figure 2 shows the contraction portion of a pupil light reflex including the position, velocity, and acceleration of the right pupil from a single subject (SA), before and after filtering the velocity data only. The characteristic of the Gaussian filter that was applied (function filtfilt.m; Matlab, ver. 5.3; The MathWorks, Inc.) varied, depending on the data sampling. Details of the exact filtering procedure used will be presented in the Results section. The time of onset of pupil contraction is shown and corresponded to when the pupil acceleration was maximally negative. The time segment when the maximum change or slope in velocity occurred (greatest absolute acceleration) was quite symmetric (almost linear), allowing this time point to be resistant to distortion and shifting by Gaussian filtering. Note that the trough in the acceleration tracing could be correctly identified only after filtering of the velocity tracing.

RESULTS

Figure 3 shows a variety of tracings recorded in the right pupil of a single subject (RK) at different stimulus intensities. A relatively longer latency (dashed arrow) was associated with relatively lower contraction amplitude (dashed double-headed arrow). In the series of increasing contraction amplitudes (see tracings between the dashed and thick solid traces), pupil light reflexes with shorter latencies (solid arrow) were mostly associated with pupil movements of greater amplitude up to the point at which the latency reached a minimum (see vertically oriented dots on traces). The inverse relationship between latency and pupil contraction was nonlinear in the brightest range of stimulus intensity, at which the contraction amplitude continued to increase, but the latency did not shorten further. Resolving slight changes in latency was more difficult with 60-Hz sampling, because the shortest time interval possible between measurement points was only 16.7 ms (relatively large time grid).

Considering the time resolution constraints of the 60-Hz sampling, we set out to determine whether a higher sampling rate (denser time grid) would improve the accuracy for measuring latency. Each panel in Figure 4 denotes the right pupil versus the left pupil contraction latency recorded simultaneously from approximately 80 light stimuli at different sampling rates (Fig. 4, open circles) that may superimpose in a single subject (LB). The filled circles represent the mean of the eight pupil light reflexes recorded from each light intensity. A regression-fitting line is added to each scatterplot to show how each sampling density grid influenced the accuracy of the relationship between right and left pupil latencies. A correlation coefficient (R^2) of 1 would mean a perfect symmetry

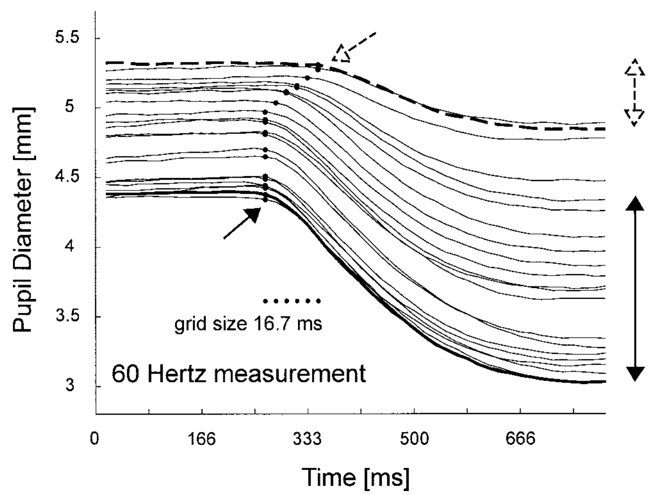

FIGURE 3. Series of right pupil light reflexes recorded at 60 Hz and in response to differing intensities of light (2-log-unit range) showing the differential effect on latency and contraction amplitude. The series of pupil light reflexes in response to lower intensities showed less contraction amplitude (*double-headed dashed arrow*) and the contraction onset (*solid dots*) corresponding to the latency came at a progressively earlier time (*diagonal linear pattern of dots*). However, as the stimulus intensity became brighter, the contraction onset did not shorten appreciably (*vertical linear pattern of dots*), Despite the increasing contraction amplitude (*double-headed solid arrow*), indicating a nonlinear effect of stimulus intensity on latency with brighter lights.

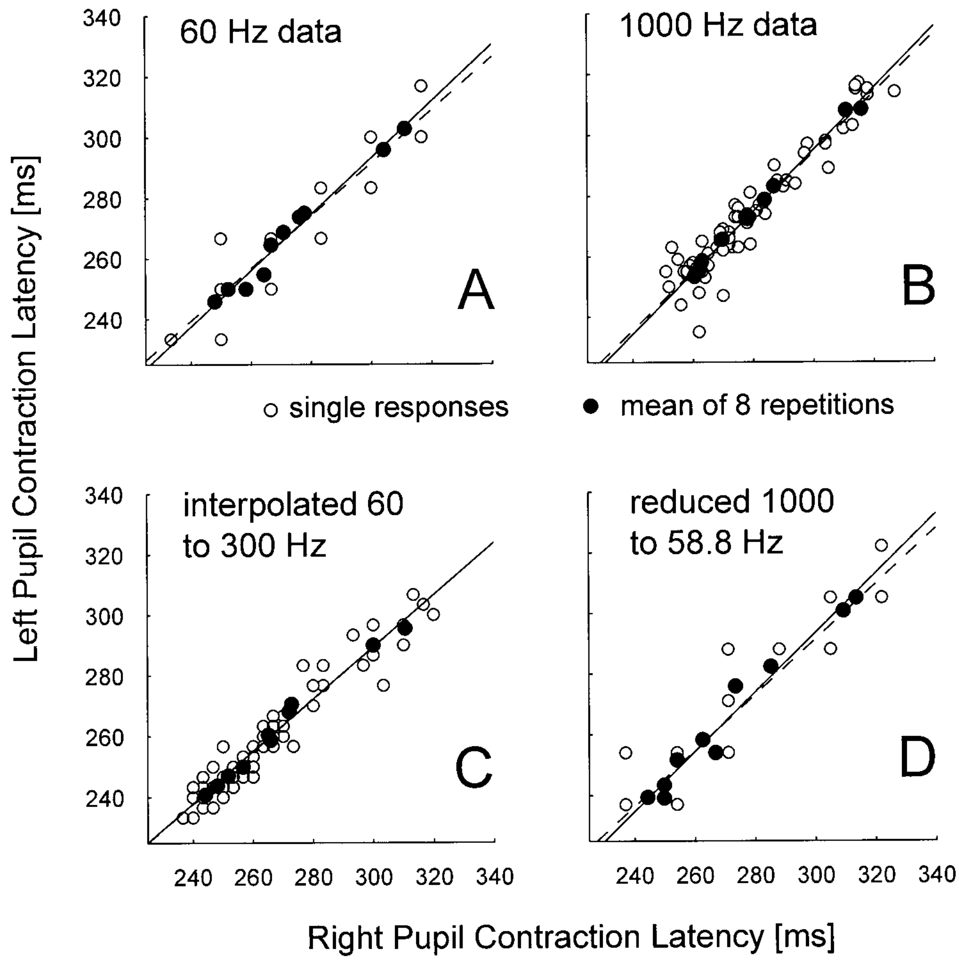

FIGURE 4. Series of linear correlations comparing the latency of the right and left pupils recorded simultaneously in one typical normal subject at multiple light intensities applied to the right and left eyes (eight repetitions per intensity and eye). In each panel, the linear correlation is shown for all 80 reflexes (*open circles* and *dashed line*) and also for the mean latency derived from each set of eight light reflexes at the five stimulus intensities applied to each eye (10 *filled circles* and *solid line*). *Circles* at data points with the same latency are superimposed. Four different data samples for the right versus left pupil latencies are shown: the video recording of data at 60-Hz (**A**), the 1000-Hz data derived from the photodiode (**B**), the interpolated data at 60 to 300 Hz (**C**), and the reduced 1000- to 58.8-Hz data (**D**). The correlation of latency between the right and left pupils was better when the eight reflexes for each stimulus intensity were averaged. Note that the measurement grid of the latencies for single pupil light reflexes varies in each panel, depending on the sample frequency.

between all the right and left pupil latencies measured. When we compared the mean of the eight pupil light reflexes derived from each intensity, the data points (Fig. 4, filled circles) showed a tighter linear distribution at all sampling rates. This was particularly apparent for the 60-Hz sampling, showing that averaging latencies of multiple pupil light reflexes helped to improve resolution of latency, because the average latency of the eight individual light reflexes was not constrained to a time grid of 16.7 ms.

We used the correlation coefficient (R^2) as a measurement-reliability tool for latency, assuming that in normal subjects, the relationship between right and left pupil latencies would correlate almost perfectly. Therefore, an optimal method of latency determination would be reflected in the highest correlation coefficient between the right and the left pupil latencies. Figure 5 shows the spectrum of increasing filtering weight applied to the velocity traces and its effect on the interpupil symmetry of latency measurements. With increasing power of

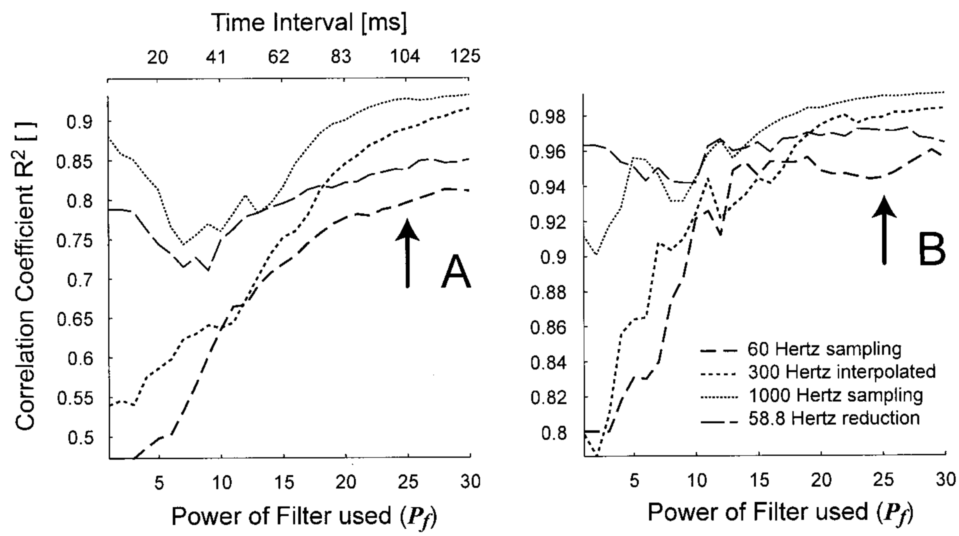

FIGURE 5. Influence of the Gaussian filter weight of the velocity traces on the right-to-left pupil symmetry of latency (represented by the correlation coefficient R^2). For each frequency, stronger filtering provided higher correlation, using all the single measurements (**A**) or the mean of eight repetitions (**B**). Each *line* represents the mean results of all seven subjects. Higher-power filtering is shown by higher numbers on the *x*-axis. The scale at the *top* of (**A**) shows the approximate corresponding interval of time over which the filter power was applied. For exact calculation of the Gaussian filter, see the Appendix. The arbitrarily selected position of the *arrow* indicates the area in which optimal filtering can be assumed.

TABLE 1. Statistical Evaluation of the Right to Left Pupil Latency

	Mean of R^2	Minimum	Maximum	SD	*P*
7 Subjects					
Single measures					
60 Hz	**0.790**	0.538	0.872	0.114	
300 Hz	0.885	0.824	0.934	0.042	0.051
1000 Hz	**0.925**	0.903	0.968	0.023	**0.024**
58.8 Hz	0.838	0.771	0.913	0.054	Not tested
Means of repetitions					
60 Hz	0.944	0.780	0.982	0.073	
300 Hz	0.978	0.957	0.993	0.012	0.23
1000 Hz	0.990	0.984	0.999	0.006	0.16
58.8 Hz	0.972	0.935	0.991	0.019	Not tested
49 Subjects					
Single measures					
60 Hz	**0.876**	0.752	0.945	0.042	
300 Hz	**0.888**	0.802	0.947	0.037	**<0.001**
Means of repetitions					
60 Hz	0.982	0.925	0.997	0.012	
300 Hz	0.981	0.922	0.998	0.014	0.62

Shown are the correlation coefficient R^2 between the original 60-Hz data and the alternative measurements derived from 7 normal subjects in one study and from 49 normal subjects in a second study.

the Gaussian filter, the time interval over which the moving filter was applied also increased. Optimal filtering for all four frequencies studied occurred when the power of filter (P_f) used was approximately 25 (Fig. 5, arrow; for a detailed methodology see the Appendix).

We then compared the 60-, 1000-, 300-, and 58.8-Hz data obtained from the seven normal subjects (Table 1). When all pupil light reflexes were assessed (not the mean of eight repetitions), the seven subjects' combined correlation coefficient was lowest in the 60-Hz and highest in the 1000-Hz measurement, resulting in a significant difference ($P < 0.05$). The R^2 of the 300-Hz data was higher than that of the 60-Hz data but the difference did not reach significance. When the mean of the eight repetitions of each eye was used for the linear regressions (Fig. 4, filled circles), the correlation coefficients all increased and were high.

These results lead to the conclusion that an increase in the accuracy of the latency determination occurs with interpolation of the 60-Hz data to 300 Hz and averaging of repetitions. The 1000- to 58.8-Hz reduced photodiode data were comparable with the original 60-Hz measurement. The different principles of the two testing methods (video camera versus photodiode) did not influence the result. In addition, the lack of perfect symmetry between right and left pupil latency, even with averaging multiple reflexes (e.g., $R^2 < 1.0$ in all groups) might be better explained by small biological variations in the latency that may be present between the direct and consensual pupil reflex and not necessarily by measurement noise, because it was found by two independent methods of measurement: video and photodiode recording.

Obtaining the arithmetic mean of the latency determined from multiple pupillary light reflexes improved the R^2 and therefore the reliability and accuracy in interpupil symmetry (Fig. 4, Table 1). We determined the effect of the number of pupil light reflexes analyzed (and averaged) on the correlation coefficient R^2 between the right and left pupil latencies. As the number of light stimuli that were used for the determination of the mean latency became less than four, the correlation coefficient R^2 began to decrease (Fig. 6), depending on the data collection group (60 or 58.8 Hz). The 1000-Hz data showed the best right–left pupil correlation of all numbers of light stimuli given (one to eight repetitions) compared with the other groups. From this analysis, it is concluded that at least four valid stimulus repetitions should be performed to overcome the rather coarse time resolution of 16.7 ms available from the 60-Hz data frequency.

For a better estimation of the variability of the latency, 60-Hz pupil recordings in 49 healthy subjects were analyzed (four repetitions per eye tested at seven different intensities over a 3-log-unit range). The result of interpupil symmetry of the 49 normal subjects in Table 1 confirmed the outcome that was obtained from the 7 normal subjects. There was a highly significant ($P < 0.001$) improvement in the right-to-left pupil correlation in the 300-Hz interpolated data compared with the

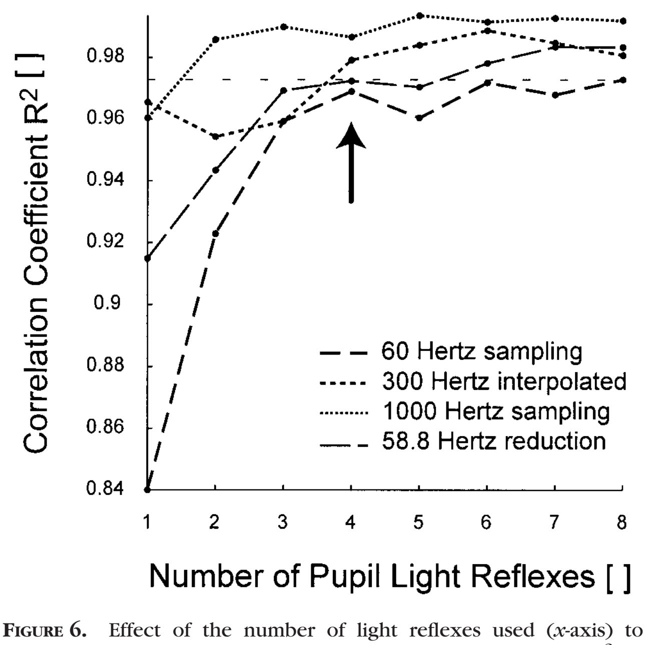

FIGURE 6. Effect of the number of light reflexes used (*x*-axis) to determine the average latency on the correlation coefficient (R^2, *y*-axis) between the right- and left-pupil latencies. The correlation between the two pupils served as an indicator of the precision of the latency determination and increased when more latencies were averaged. If more than four repetitions were measured, the correlation remained stable in all frequency groups. The precision of measuring eight times at 60 Hz could be achieved by measuring 300 Hz for only four times (*horizontal dashed line*). The *lines* represent the medians of four normal subjects in whom more than 70 pupil responses of a possible 80 were obtained that were measurable.

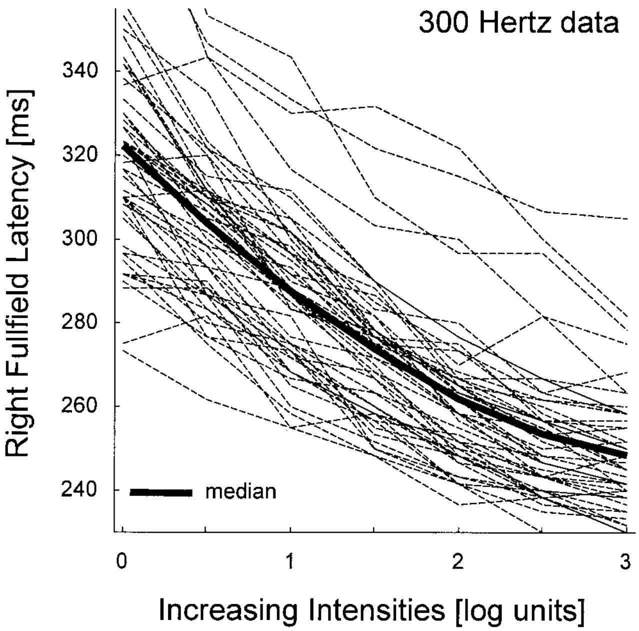

FIGURE 7. The effect of log stimulus intensity (administered to the right eye) on latency is shown for 49 normal eyes (*solid thick line*: median response for all subjects; *dashed lines*: individual subjects) over a 3-log-unit intensity range (from 30 dB attenuation [37 asb] to 0 dB attenuation [37,000 asb]). Lower stimulus intensities corresponded to a greater intersubject variability in latency (69 ms), and higher intensities corresponded to a lower intersubject variability in latency (38 ms). Theoretically, it would take almost a 2-log-unit change in stimulus intensity (or retinal sensitivity) to account for the range in latency observed between subjects, based on the median line shown.

60-Hz data. However, when the mean latency of eight measurements was calculated (eight each from the right and left pupils when four stimuli were given to each eye), the 60-Hz data on the right pupil versus left pupil latency correlation (R^2) was not statistically distinguishable from the 300-Hz data.

The results in the 49 normal subjects indicated that pupil latency can substantially differ from one person to one another. Figure 7 summarizes the traces from all 49 subjects obtained from right full-field stimulation within a range of light intensities of 3 log units. The median of all latencies measured at each intensity (Fig. 7, solid line) shortened from 322 ms at the lowest intensity to 248 ms at the brightest intensity (difference: 74 ms). At a given intensity, the range of the latency varied considerably among the 49 subjects. For example, the range of latency for 90% of the subjects was between 230 and 268 ms (intersubject range: 38 ms) at the highest intensity and was between 288 and 357 ms (intersubject range: 69 ms) at the lowest intensity. The amount of change in retinal illumination (retinal sensitivity) that would be required to explain such variation would be equivalent to 2 to 2.5 log units, based on the median curve, which related log stimulus intensity to latency.

From the data of the 49 normal subjects, right and left pupil traces were averaged together to investigate the latency difference between the right- and left-eye stimulations, for both the 60- and 300-Hz data and also for a third data set, in which only every second time point of the 60-Hz data was considered, resulting in a frequency reduction to 30 Hz. The variability in the intereye difference in latency due to the afferent input appeared greater at the lower stimulus intensities. This is further characterized in Figure 8A, which shows the absolute value of the intereye difference in latency (300 Hz data) with the 95th percentile to be 35 ms at the lowest intensity and 8.3 ms at the highest intensity. The values between intensities are located on an exponential function. Figures 8B and 8C show estimates of the same 95th-, 90th-, and 50th-percentile range for intereye latency in normal subjects, using the 60-Hz measurement and the 30-Hz reduction. The potential clinical usefulness of the latency in identifying asymmetric input to the right and left eyes is demonstrated by examples from three patients with unilateral optic neuritis added to the panels (represented by stars, circles, and triangles). The intereye latency difference clearly exceeded the 95th percentile of the normal population and was maximally differentiated from normal intereye asymmetry in the 300-Hz interpolated data at all intensities.

DISCUSSION

This study provided insight into analysis strategies that could be successfully applied to optimize the measurement of latency of the pupillary light reflex in normal subjects. First, the results showed that when more stimuli, hence, reflexes, were available to obtain the mean latency, the precision was greater (Fig. 6). For example, at a recording rate of 60 Hz, measurement variability became noticeably worse when the number of pupil light reflexes used to derive mean latency was reduced to less than four binocular pupil recordings. A higher sampling rate of 1000 Hz improved the resolution of latency, and the filtering reduced the high-frequency content of the pupil trace. A very high sampling rate may not be necessary to reproduce a low-frequency component of the pupil movement. A system with higher spatial resolution for the measurement of the pupil diameter could be even more effective than a very high sampling rate system with low single-measurement precision of pupil diameter. Interpolation of the 60-Hz video recording to 300 Hz enhanced the accuracy of latency determination, because the sampling interval was reduced and the computation of gradients was performed on discrete data points. This finding is in agreement with another study suggesting that data from a sampling frequency lower than 60 Hz can be improved.[24] It seems that the effect of using a higher sampling frequency can also be achieved by interpolating the 60-Hz curve or averaging the latencies derived from four alternating stimuli while recording both the right and left pupils.

An improved method for determining the time of contraction onset of the pupil light reflex is desirable for evaluating its utility in diagnosing disease, and this was one of the main goals of the current study. In earlier studies of pupil latency measurements, a certain amount (criterion) of contraction amplitude was proposed to determine the onset of the reflex (amplitude threshold crossing).[23] However, this approach depends on the movement range of the pupil and is limited by iris mechanics. The onset of contraction determined by this criterion could be delayed solely by a small pupil that has limited range of movement. Therefore, this criterion is dependent on the amount of pupil movement and is not directly related to the actual starting time of the pupil movement. Also, the use of velocity as a criterion for defining the onset of the pupil light reflex (velocity threshold crossing)[24,29] is influenced by the amount of contraction amplitude, because contraction amplitude and velocity are closely correlated and dependent on pupil size and range of movement. A third approach has used the intersection of two straight-line fits[28,34] (one during the baseline, or latent, period and one during the contraction phase of the pupil light reflex). This method can be influenced by the degree of pupil movement preceding the onset of contraction and the slope of the contraction's velocity, which may independently vary from the true latency.

We have used the absolute minimum of the derivative of the velocity trace, acceleration, in this study (Fig. 2) and pre-

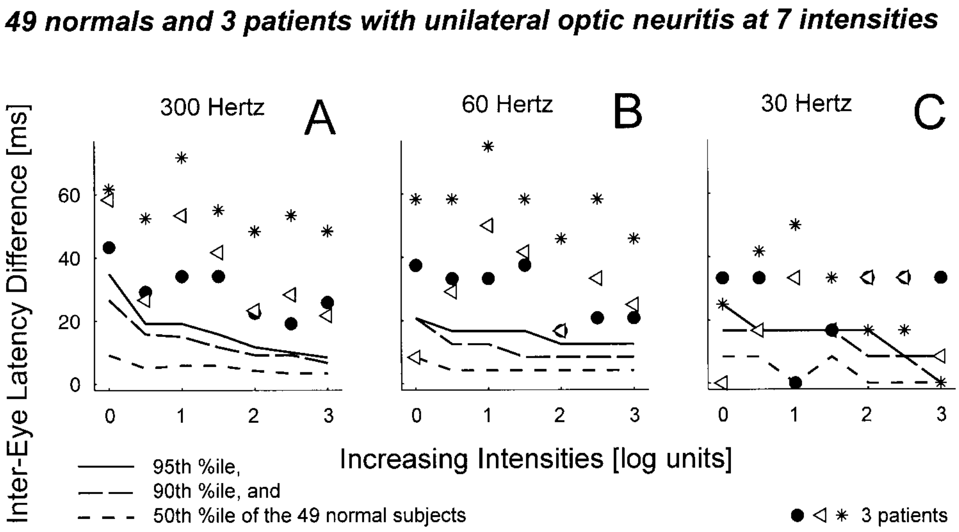

FIGURE 8. Effect of stimulus intensity on the normal intereye latency difference in afferent pupil input, described as percentiles of the 49 normal subjects. In the 300 Hz (**A**), the 95th percentile line ranged from 35 ms at the lowest intensity to 8.3 ms at the highest intensity. Similarly, the 90th and 50th percentiles exponentially decreased with increasing stimulus intensities. The 60-Hz (**B**) and 30-Hz data (**C**) revealed similar patterns between intensities, but not as clearly delineated as with the 300-Hz data. The potential for identifying patients with unequal afferent visual input is also shown for three patients (denoted by *stars*, *circles*, and *triangles*). Almost all the intereye latency differences were outside the 95th percentile for normal subjects.

viously,[33] because it does not rely on the use of arbitrary thresholds for determining the onset of contraction. Because the acceleration definition of the onset of contraction really represents where the change in pupil size (velocity) differs the most (absolute maximum acceleration), we believe it is a more appropriate definition of the onset of contraction and more reliably reflects the latency of the pupil light reflex.

Limitations on the bit resolution of pupil size in a given instrument (y-axis of the pupil trace) may also confound the correct determination of latency. Bit resolution relates to the smallest change in pupil size that can be resolved by a given instrument's hardware and, in this case, the sampling or representation of the pupil size measured. Filtering of digitally sampled data may provide a better approximation of the true biological movement of the iris, which is relatively slow because of the properties of smooth muscle. As shown in Figure 9, the latency would be incorrectly predicted by using only the digital raw position data without filtering. The choice of an optimal filter is not trivial, either. In contrast to the Gaussian filter, the Savitzky-Golay filter[39] is capable of assigning a pupil diameter that is actually greater than or less than the raw bit-sampled data value. This filter works noniteratively and is a simple mathematical tool that consists of a moving polynomial filter. The size of the moving window (five time points in this study) and the order of the polynomial fit (second order) can be varied to optimally reflect the true biological movement. The use of the Savitzky-Golay filter is recommended for video-sampled pupil data, because it does not apply an abrupt frequency cutoff and, although it effectively filters high-frequency noise, it also preserves the low-frequency component of the biological slow movement of the pupil.

The improved technique developed in this study for better determination of latency was further applied to a larger data set from 49 normal subjects to improve understanding of how latency varies in response to changing stimulus intensity and among individuals. Pupil latency became shorter as a function of light intensity in a predictable, nonlinear fashion, showing less change at higher intensities, as confirmed by others.[40] The latent period is composed of two separate mechanisms: an irreducible minimal latent period built into the motor system of the iris and a variable additional delay due mainly to the retinal discharges and their temporal summation that is processed in the midbrain (pretectal olivary nucleus)—the weaker the stimulus, the longer the latent period. The relationship between sensory stimulus and delay applies not only to the pupillary light reflex, but also to many other reflexes.[11] The relationship of latency as a function of log intensity is reproducible in a given eye and is similar for the input of the right and left eyes of a normal subject. However, there was considerable interindividual variability of pupil latency as a function of intensity in

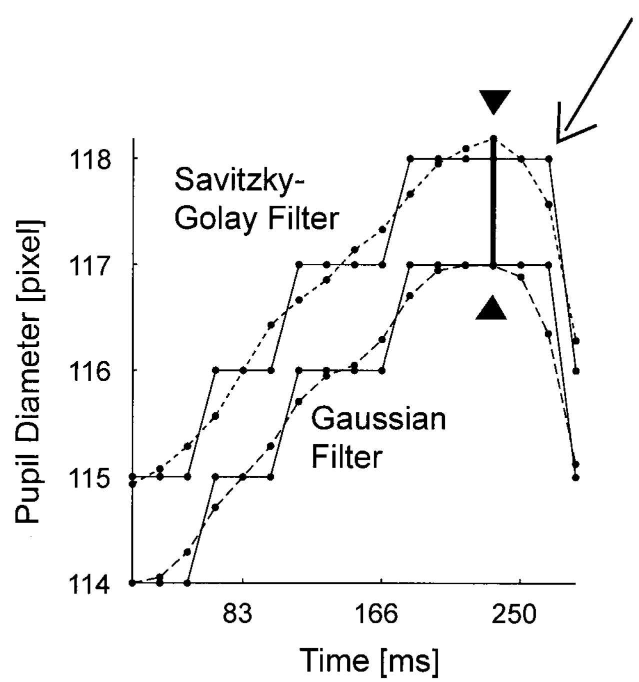

FIGURE 9. Errors in the determination of latency that can occur in raw unfiltered data due to the effect of bit-sampling constraints. The unfiltered raw tracing recorded is shown twice as the *solid line* connecting the small *filled circles* where the pupil size can change by only one arbitrary bit unit (for clarification purposes, data with 8-bit resolution are shown on the y-axis, although most systems for pupil measurement generate analog data that are sampled with 12-bit resolution). The *top raw trace* was filtered by a Savitzky-Golay filter, which is a mathematical, noniterative tool using a moving polynomial smoothing. This replicates the expected smooth muscle movement of the pupil and may assume a pupil size smaller or larger than the raw data. The *bottom raw tracing* was filtered by a Gaussian filter that cannot exceed the maximum of the raw tracing. *Arrow*: onset of contraction in the raw tracing. The better estimated onset of contraction in the filtered traces occurred two time-points (33.3 ms) earlier, as identified by the *vertical line* between the *two arrowheads*.

a given eye. This effectively reduces the sensitivity of latency for diagnosing abnormal input deficits in an individual eye of a patient, unless the input deficit is large enough to exceed the normal interindividual variation in pupil latency. The reason for the large range in latency measured among different individuals under the same stimulus conditions is not obvious. The source of the shift, or offset of latency, observed in different individuals could occur at the afferent processing of the light reflex (retina or optic nerve), at the interneuron or pretectal nucleus, or at the efferent pathway from the Edinger-Westphal nucleus, up to and including the iris sphincter muscle.

The results from the normal subjects also showed that the asymmetry of latency between the input of the right and left eyes of an individual is relatively small, especially at moderate or higher stimulus intensities. We provided evidence that the normal range of intereye asymmetry in latency was 8.3 ms at the highest intensity and 35 ms at the lower intensities, and that asymmetry in patients with afferent disease may fall outside normal limits. To the best of our knowledge it has not been reported that intereye difference in latency is wider at lower stimulus intensities in normal subjects. This relatively slight variation of the intereye difference in latency is very likely to provide a useful clinical parameter that would supplement the measurement of the relative afferent pupil defect, as shown in Figure 8. Future studies will focus on which intensity range of light stimulus is most sensitive for detecting the asymmetry of timing of pupil input outside the range of normal subjects that is due to diseases affecting the afferent visual system.

Acknowledgments

The authors thank Mike Rosenberg, Andreas Schötzau, and Thomas Haslwanter for sharing their experience and Paula Moore, Chad Denison, Stacy Thompson, and Aki Kawasaki for providing expert assistance in collecting pupil recordings.

References

1. Schubert E, Thoss F. Influence of different adaptation on the threshold as well as the stimulus strength dependency of latency and amplitude in the human consensual pupillary reflex [in German]. *Pflugers Arch Gesamte Physiol Menschen Tiere.* 1967;294:28–39.
2. Halliday AM, McDonald WI, Mushin J. Delayed visual evoked response in optic neuritis. *Lancet.* 1972;7758(1):982–985.
3. Diener HC, Scheibler H. Follow-up studies of visual potentials in multiple sclerosis evoked by checkerboard and foveal stimulation. *Electroencephalogr Clin Neurophysiol.* 1980;49:490–496.
4. Cox TA, Thompson HS, Hayreh SS, et al. Visual evoked potential and pupillary signs: a comparison in optic nerve disease. *Arch Ophthalmol.* 1982;100:1603–1607.
5. Frederiksen JL, Petrera J. Serial visual evoked potentials in 90 untreated patients with acute optic neuritis. *Surv Ophthalmol.* 1999;44(suppl 1):S54–S62.
6. Pulfrich C. Die Stereoskopie im Dienste der isochromen und heterochromen Photometrie. *Naturwissenschaften* (*Berlin*). 1922; 10:553–564; 569–574; 596–601; 714–722; 735–743; 751–761.
7. Nickalls RW. The rotating Pulfrich effect, and a new method of determining visual latency differences. *Vision Res.* 1986;26:367–372.
8. Diaper CJ. Pulfrich revisited. *Surv Ophthalmol.* 1997;41:493–499.
9. Mojon DS, Rosler KM, Oetliker H. A bedside test to determine motion stereopsis using the Pulfrich phenomenon. *Ophthalmology.* 1998;105:1337–1344.
10. Loewenfeld IE, Newsome DA. Iris mechanics. I. Influence of pupil size on dynamics of pupillary movements. *Am J Ophthalmol.* 1971;71:347–362.
11. Loewenfeld IE. The light reflex: IV. Factors related to retinal physiology and to the pupillary motor system. A. Latent periods. In: Butterworth H, ed. *The Pupil: Anatomy, Physiology and Clinical Applications*. Boston: Butterworth Heinemann; 1999:158–171.
12. Miller SD, Thompson HS. Pupil cycle time in optic neuritis. *Am J Ophthalmol*. 1978;85:635–642.
13. Jakobsen J. Pupillary function in multiple sclerosis. *Acta Neurol Scand.* 1990;82:392–395.
14. van Diemen HA, van Dongen MM, Nauta JJ, et al. Pupillary light reflex latency in patients with multiple sclerosis. *Electroencephalogr Clin Neurophysiol.* 1992;82:213–219.
15. Lüdtke H, Kriegbaum C, Leo-Kottler B, et al. Pupillary light reflexes in patients with Leber's hereditary optic neuropathy. *Graefes Arch Clin Exp Ophthalmol.* 1999;237:207–211.
16. Kase M, Nagata R, Yoshida A, et al. Pupillary light reflex in amblyopia. *Invest Ophthalmol Vis Sci.* 1984;25:467–471.
17. Barbur JL, Hess RF, Pinney HD. Pupillary function in human amblyopia. *Ophthalmic Physiol Opt.* 1994;14:139–149.
18. Alexandridis E, Argyropoulos T, Krastel H. The latent period of the pupil light reflex in lesions of the optic nerve. *Ophthalmologica.* 1981;182:211–217.
19. Lanting P, Bos JE, Aartsen J, et al. Assessment of pupillary light reflex latency and darkness adapted pupil size in control subjects and in diabetic patients with and without cardiovascular autonomic neuropathy. *J Neurol Neurosurg Psychiatry.* 1990;53:912–914.
20. Pfeifer MA, Weinberg CR, Cook DL, et al. Correlations among autonomic, sensory, and motor neural function tests in untreated non-insulin-dependent diabetic individuals. *Diabetes Care.* 1985; 8:576–584.
21. Listing JB. Beitrag zur physiologischen Optik. In: Engelmann W, ed. *Ostwald's Klassiker der Exakten Wissenschaften ed.* Leipzig, Germany: Göttinger Studien; 1845: Reprinted in 1905 as No. 147.
22. Alpern M. The relationship of visual latency to intensity. *Arch Ophthalmol.* 1954;51:369–374.
23. Lowenstein O, Kawabata H, Loewenfeld IE. The pupil as an indicator of retinal activity. *Am J Ophthalmol.* 1964;57:569–596.
24. Bos JE. Detection of the pupil constriction latency. *Med Biol Eng Comput.* 1991;29:529–534.
25. Myers GA, Stark L. Level dependent signal flow in the light pupil reflex. I. Latency of time domain responses to transient stimuli. *Biol Cybern.* 1993;68:229–234.
26. Bergamin O, Schötzau A, Turtschi S, et al. Age, gender and test location in pupil perimetry. In: Wall M, Heijl A, eds. *Perimetry Update 1996/97.* Proceedings of the XIIth International Visual Field Symposium, Würzburg, Germany. Amsterdam: Kugler Publications; 1997:59–65.
27. Bergamin O, Lemola K, Zulauf M. Adaption phenomenon in pupil perimetry. In: Wall M, Mills RP, eds. *Perimetry Update 2000/2001.* Proceedings of the XIVth International Visual Field Symposium, Halifax, Canada. Kugler Publications, The Hague, Netherlands; 2001:121–129.
28. Alpern M, McCready DW, Baar L. The dependence of the photopupil response on flash duration and intensity. *J Gen Physiol.* 1963;47:265–278.
29. Feinberg R, Podolak E. Latency of pupillary reflex to light stimulation and its relationship to aging. In: Welford AT, Birren RH, Thomas CC, eds. *Behavior, Aging and the Nervous System*. Springfeld, IL: Thomas; 1965:326–339.
30. Lee RE, Cohen GH, Boynton RM. Latency variation in human pupil contraction due to stimulus luminance and/or adaptation level. *J Opt Soc Am*. 1969;59:97–103.
31. Cibis GW, Campos EC, Aulhorn E. Pupillomotor latent period. *Vision Res.* 1977;17:737–738.
32. Pfeifer MA, Cook D, Brodsky J, et al. Quantitative evaluation of sympathetic and parasympathetic control of iris function. *Diabetes Care.* 1982;5:518–528.
33. Kardon RH, Kirkali PA, Thompson HS. Automated pupil perimetry: pupil field mapping in patients and normal subjects. *Ophthalmology.* 1991;98:485–495.
34. Bergamin O, Schötzau A, Sugimoto K, et al. The influence of iris color on the pupillary light reflex. *Graefes Arch Clin Exp Ophthalmol.* 1998;236:567–570.

35. Hong S, Narkiewicz J, Kardon RH. Comparison of pupil perimetry and visual perimetry in normal eyes: decibel sensitivity and variability. *Invest Ophthalmol Vis Sci.* 2001;42:957–965.
36. Zabriskie NA, Kardon RH. The pupil photostress test. *Ophthalmology.* 1994;101:1122–1130.
37. Kawasaki A, Moore P, Kardon RH. Variability of the relative afferent pupillary defect. *Am J Ophthalmol.* 1995;120:622–633.
38. Kawasaki A, Moore P, Kardon RH. Long-term fluctuation of relative afferent pupillary defect in subjects with normal visual function. *Am J Ophthalmol.* 1996;122:875–882.
39. Savitzky A, Golay MJE. Smoothing and differentiation of data by simplified least squares procedures. *Anal Chem.* 1964;36:1627–1639.
40. Ellis CJ. The pupillary light reflex in normal subjects. *Br J Ophthalmol.* 1981;65:754–759.

Appendix

Figure 5 shows the effect of the increasing power of the Gaussian filter (P_f) to the velocity traces. To obtain a frequency modulated Gaussian array that can be used for filtering, the following calculations were necessary. For f_s = 300 Hz and P_f = 5, for example, the Gaussian distribution gf_{peak1} resulted in

$$gf_{peak1}\ (n = 1 \text{ to } p) = e^{-([2\cdot(n-c)]/w)^2}$$
$$= (0.0307, 0.4185, 1.0000, 0.4185, 0.0307, 0.0004)$$

where $w = f_s \cdot P_f \div 700$; $p = \{3 \cdot w\}$; and $c = \{p \div 2\}$, with {} denoting rounding to the next integer. Only an array with a total sum of 1 (gf_{sum1}) is useful for smoothing purposes. For the 300-Hz velocity tracing, gf_{sum1} would be the resultant Gaussian filter if the chosen filter power P_f was optimal

$$gf_{sum1} = gf_{peak1}/\text{sum}\ (gf_{peak1})$$
$$= gf_{peak1}/1.8962$$
$$= (0.0160, 0.2202, 0.5274, 0.2202, 0.0160, 0.0002)$$

The approximate time span of the applied filter can be calculated by the length of the array gf_{sum1} (or gf_{peak1}) multiplied by the time grid of the applied frequency (300 Hz): $6 \cdot 3.33$ ms = 20 ms.